

# Numerical Simulation of Seismic Slope Stability Analysis Based on Tension-Shear Failure Mechanism

Yingbin Zhang<sup>1</sup>, Guangqi Chen<sup>1\*</sup>, Jian Wu<sup>1</sup>, Lu Zheng<sup>1</sup>, Xiaoying Zhuang<sup>2</sup>

<sup>1</sup>Department of Civil and Structure Engineering, Kyushu University, Fukuoka, JAPAN

<sup>2</sup>Department of Geotechnical Engineering, Tongji University, Shanghai, CHINA

E-mail: yingbinz719@126.com, chen@civil.kyushu-u.ac.jp (\*Corresponding author)

**ABSTRACT:** Most slope stability analysis approaches regard the failure mechanism of seismic slope as single shear failure while ignoring the influence of tension failure. However, many model testes and a large number of post-earthquake investigations provided supporting evidence of the significant influence of tension failure in seismic slope instability. To estimate the effects of tension failure on seismic slope stability, a numerical modeling considering both shear and tension failure is performed using FLAC<sup>3D</sup>. After discussions of failure mechanism, strength reduction techniques and the definition of slope failure, a homogeneity slope under a modified transverse earthquake load is analyzed. The results obtained from the simulation are presented in terms of permanent displacement, factor of safety and failure surface. Finally, the outcomes compared with those from various existing methods. The results show that the influence of tension failure is significant and consideration of it is necessary.

**KEYWORDS:** Seismic slope stability analysis, Numerical simulation, Failure mechanism, Tension failure, Factor of safety.

## 1. INTRODUCTION

Landslide is one of the worst natural disasters. As one of the main trigger, the earthquake can easily induce collapse of slopes and produce landslides that can result in serious damage to life and property. For example, the Wenchuan earthquake (Ms=8.0) occurred in Sichuan Province, China at 14:28 CST on 12 May 2008 induced as many as 56,000 landslides [1]. It is estimated that over one third of the total lost from the 2008 Wenchuan earthquake was caused by the earthquake induced landslides. Hence, the evaluation of stability of seismic slope is the most important aspect of geotechnical earthquake engineering, especially when the slopes are situated close to residential areas.

There are at least four different formulations of the seismic slope stability analysis problem: in terms of (1) the factor of safety  $F$ , (2) the critical seismic coefficient  $k_c$ , (3) the permanent displacement  $D$ , and (4) the shape of slip surface. In order to solve these problems, several methods can be used in evaluating the stability of slopes subject to earthquake loading. These methods can fall into three general categories: (1) pseudo-static method, (2) permanent displacement method, and (3) stress-strain method. Each of these types of analysis has strengths and weaknesses, and each can be appropriately applied in different situations [2]. These methods are briefly retrospective as follow:

The majority of seismic slope stability analyses performed in practice still use pseudo-static approaches where the effect of earthquake on a potential failure soil mass is represented in an approximate manner by a static force. As we know, magnitude, direction and point of application are three elements of a force. In generally, the pseudo-static force equal to the product of the gravitational force and a coefficient,  $k$ , the pseudo-static seismic coefficient and act on the center of gravity of a potential sliding mass or of a typical vertical slice in various slice method at horizontal direction. Pseudo-static has been studied by many researchers in the aspects of magnitude, direction and point of application of pseudo-static force, respectively. Firstly, because magnitude of the pseudo-static force on a mass of weight  $W$  is  $kW$ , selection of the pseudo-static coefficient  $k$  is the most important aspect of pseudo-static method. Some researcher proposed many useful studies. Table 1 lists several recommendations for selecting a pseudo-static coefficient. Secondly, analyses performed by several investigators with an inclined seismic force (i.e. coupled with vertical component of the earthquake force) have shown that the inclination can have a significant influence on the seismic slope stability analysis [11, 12]. Thirdly, different points of application of pseudo-static force can induce a significant difference in the result. Seed [4] provided a well-known example, the analysis of Sheffield

Dam. In his study the seismic forces were applied at the base and the center of gravity of each slice, respectively, and the results of factor of safety were 1.21 and 1.32, respectively. Pseudo-static method can be simply and directly used to identify the factor of safety  $F$  and the critical seismic coefficient  $k_c$  but it cannot simulate the transient dynamic effects of earthquake shaking, because it assumes a constant unidirectional pseudo-static acceleration. In addition, performance of slope is closely related to permanent displacement, but the results of pseudo-static method are difficult to interpret the performance of slope after a seismic event because this method provides no information about permanent displacement.

Table 1 Pseudo-static coefficient from several studies

Recommended pseudo-static coefficient ( $k/g$ )	Factor of safety	Permanent displacement ( $D/m$ )	Original application	Ref.
0.1 (R-F=IX) 0.2 (R-F=X) 0.5 (R-F=XI)	$F > 1.0$	-	Nature or man-made slope	[3]
0.1 ( $M=6.5$ ) 0.15 ( $M=8.25$ )	$F > 1.1$ 5	$< 1$	Earth dams	[4]
(1/3~1/2)PGA	$F > 1.0$	-	-	[5]
1/2 PGA 1/2 PGA ( $M=8.25$ ) 1/3 PGA ( $M=7.5$ ) 1/4 PGA ( $M=7.0$ ) 1/5 PGA ( $M=6.5$ )	$F > 1.0$	$< 1$	Earth dams	[6]
0.15	$F > 1.1$	-	Dams	[8]
(0.6~0.75) PGA <sub>rock</sub>	$F > 1.0$	$< 0.15 \sim 0.3$	Soild-waste landslides	[9]
(0.25~0.75) PGA <sub>rock</sub>	$F > 1.0$	$< 0.05 \sim 0.15$	Urbanized slopes	[10]

Note: R-F is Rossi-Forel earthquake intensity scale, IX: severe earthquake, X destructive earthquake, XI catastrophic earthquake;  $M$  is earthquake magnitude; PGA is peak ground acceleration, in terms of acceleration of gravity.

Permanent displacement is a useful index of slope performance, especially for those man-made slopes constructed for special

purposes like dams, embankments, etc. Newmark's method provides a measure of permanent displacement along a fixed slip surface based on a double integration of acceleration of a potentially sliding soil block with simple input parameters and relatively low computational complexity. In fact, the Newmark's method also involves some assumptions about the manner in which the earthquake loading. Considerable attention has been focused over the last decades on developing procedures to more accurately analyze the seismic performance of a slope for dams, embankments or other important structures by modeling the dynamic slope response more rigorously. Jibson [2] grouped analytical procedures for estimating permanent co-seismic landslide displacements into three types: (1) rigid-block [13], (2) decoupled [14, 15], and (3) coupled [16-19] (see figure 1).

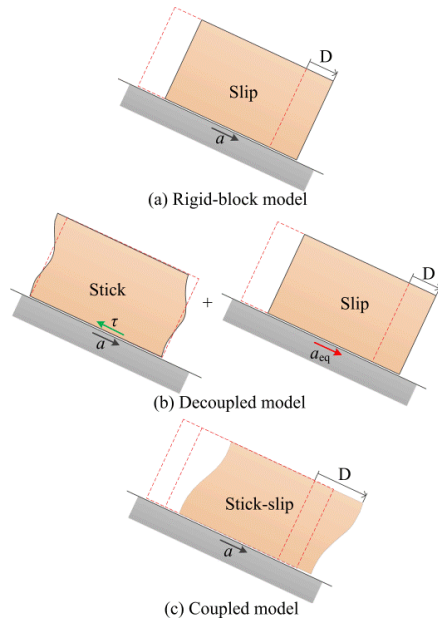


Figure 1 Calculated models of permanent displacement: (a) rigid block model, (b) decoupled model, and (c) coupled model.

Stress-strain method represents a powerful alternative approach for seismic slope stability analysis which is accurate, versatile and requires fewer a priori assumptions, especially, regarding the shape of failure surface. With the developments of computer technology and simulation approach in recent decades, the numerical simulation method is becoming used increasingly in engineering practice and more and more popular for the real dynamic analysis. The most commonly applied numerical methods can be categorized into continuous and discontinuous approach. This paper focus on homogeneity slope stability analysis, i.e. continuous slope material is assumed. Stress-strain methods have been used successful in seismic slope stability analysis by earlier researchers, e.g. finite element method (FEM) [20], finite difference method (FDM) [21, 22].

However, almost all of the above methods consider the failure mechanism of seismic slope as a completely shear failure. The frequently occurring earthquake events in recent years in New Zealand, Japan and China have led to a renewed knowledge in mechanism of instability of slopes. A large number of evidences from investigations of earthquake induced landslide and shaking table test show that tension failures appear in top of almost all landslides or potential sliding slopes. For example, Figure 2 shows steep scarp with coarse crack of Donghekou landslide and Pingxicun landslide induced by Wenchuan earthquake occurred in 2008 and Figure 3 shows a result of shaking table test carried out by Wakai et al. [23] in which tension crack can be obviously found in top of slope. The existing methods what usually only based on shear failure mechanism while ignoring the tension failure may lead to inaccuracy especially when the slope shook by a strong earthquake



(a) Steep scarp with coarse cracks of Donghekou landslide, Qingchuan



(b) Steep scarp with coarse cracks of Pingxicun landslide, Pingwu



(c) Tension cracks in the top of Shiziliang

Figure 2 Evidences of the existence of tension failure from investigation of Wenchuan earthquake induced landslides or potential landslide. Steep scarp with coarse cracks of (a) Donghekou landslide, Qingchuan and (b) Pingxicun landslide, Pingwu and (c) tension cracks in the top of Shiziliang landslide. (Adopted from reference [26])

load. There are a large number of described, analytical and numerical studies which have provided supporting evidences of the existence of tension failure in slope stability analysis. Huang et al. [24, 25], Xu et al. [26] and Yin et al. [27] have gave much detailed description for tension segment of slope failure surface based on post-earthquake investigations. Zheng et al. [21], Zhang et al. [28] and Yan et al. [29] have certificated the existing of tension failure zone by analyzing the mechanism of seismic slope using numerical simulation. Zhang et al. [30] showed that significant effect of tension failure on slope stability analysis using upper bound limit analysis. These studies, however, most focus on the description or explanation of phenomenon, but few on deep research of stability analysis subjected to the tension failure.

Hence, to investigate how the tension failure effect on seismic stability analysis, a full dynamic analysis is carried out in this paper

with an emphasis on seismic slope stability using finite difference method through a homogeneity slope.



Figure 3 Supporting evidence of the existence of tension failure from shaking test (Adopted from reference [23])

## 2. IMPORTANT ASPECTS IN SEISMIC SLOPE STABILITY ANALYSIS

In this section, three major aspects that influence seismic slope stability analysis are discussed. The first is about the failure mechanism of seismic slope. The second is the concept of factor of safety and the third is the definition of the slope failure.

### 2.1 Failure mechanism subjected to tension failure

At present, the failure mechanism of seismic slope follows the static slope failure mechanism, i.e. the main reason that caused seismic slope instable is shear failure while ignoring the influence of tension failure. In fact, with the reason of small tensile strength and the action of earthquake loading, the slope in reciprocating motion is more easily to be tensioned. Stress states of a point in slope mass at two situations, static and dynamic, are illustrated as Figure 4. As the description of most soil mechanics textbooks, compressive stresses are considered positive, and tensile stresses are negative. The major and minor principal stresses  $\sigma_1$  and  $\sigma_3$  of static state obtained from

$$\sigma_1 = \frac{\sigma_x + \sigma_z}{2} + \sqrt{\left(\frac{\sigma_x - \sigma_z}{2}\right)^2 + \tau_{xz}^2} \quad (1)$$

$$\sigma_3 = \frac{\sigma_x + \sigma_z}{2} - \sqrt{\left(\frac{\sigma_x - \sigma_z}{2}\right)^2 + \tau_{xz}^2} \quad (2)$$

Where  $\sigma_x$ ,  $\sigma_z$  are stress in horizontal and vertical direction respectively; and  $\tau_{xz}$  is shear stress.

When the slope is effecting by a horizontal earthquake loading what propagate from bottom upward to top of the slope. A shear stress  $\tau_s$  caused by the earthquake loading can added into the existing state stress state. The magnitude and direction of dynamic stress  $\tau_s$  are time dependent. If not consider the influence of wave reflection and refraction, the stress state in this situation can be simply indicated as figure 4(b). The combined major and minor principal stresses  $\sigma_1'$ ,  $\sigma_3'$  calculated from

$$\sigma_1' = \frac{\sigma_x + \sigma_z}{2} + \sqrt{\left(\frac{\sigma_x - \sigma_z}{2}\right)^2 + (\tau_{xz} + \tau_s)^2} \quad (3)$$

$$\sigma_3' = \frac{\sigma_x + \sigma_z}{2} - \sqrt{\left(\frac{\sigma_x - \sigma_z}{2}\right)^2 + (\tau_{xz} + \tau_s)^2} \quad (4)$$

where  $\tau_s$  obtained from:

$$\tau_s = \rho C_s v_s \quad (5)$$

where  $\rho$  is mass density of soil material,  $C_s$  is speed of  $s$ -wave propagation through material, and  $v_s$  is input shear particle velocity caused by earthquake loading in horizontal direction. Equations (3)

and (4) show an opposite change pattern of major and minor principal stresses  $\sigma_1'$ ,  $\sigma_3'$ . In the  $(\sigma, \tau)$  plane, this change pattern presented as expand or narrow of the Mohr circle (see figure 5).

Note that if the influence of wave reflection and refraction are considered, the expressions of major and minor principal stresses  $\sigma_1'$ ,  $\sigma_3'$  will be very complex. This point will be detail description by monitoring records through the time history of seismic excitations.

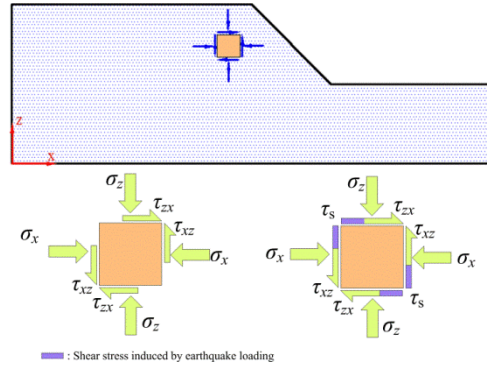


Figure 4 Stress state of a point in slope mass at conditions of (a) static and (b) horizontal seismic shear stress loadings

Many failure criteria have been presented for modeling the strength of soil, the Mohr-Coulomb criterion remains the one most widely used in geotechnical practice. A modified Mohr-Coulomb failure criterion is used in this study. The representation of the failure criterion in the  $(\sigma, \tau)$  plane is sketched in Figure 5. The failure envelope is defined from point A to B by the Mohr-Coulomb yield function

$$f_{shear} = \frac{\sigma_1' - \sigma_3'}{2} - c \cos \varphi - \frac{\sigma_1' + \sigma_3'}{2} \sin \varphi = 0 \quad (6)$$

and from B to C by the tension yield function

$$f_{tension} = \sigma_3' - \sigma_t = 0 \quad (7)$$

where  $c$  is cohesion,  $\varphi$  is friction angle of soil material,  $\sigma_t$  is tension strength of soil material.

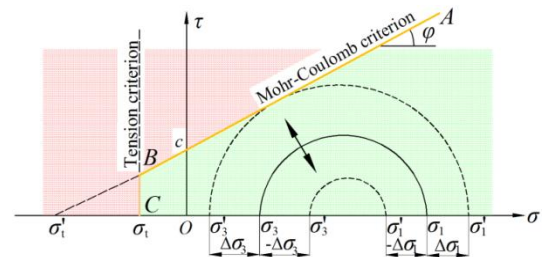


Figure 5 Failure criterion combined tension-shear failure mechanism

Because tensile strength of soil material is much smaller than their shear strength, we can take the opinion that once the minor principal stress  $\sigma_3$  equals to tensile strength  $\sigma_t$ , the tension failure will occur and the tension failure surface parallel to minor principal stress plane.

The failure functions  $f_{tension}$  and  $f_{shear}$  can be interpreted as follows

- $f_{tension} > 0$  and  $f_{shear} < 0$  note that the normal and shear stresses on a plane in a soil mass inside failure envelope, green zone in figure 5. Failure will not occur in this situation;
- $f_{tension} = 0$  or  $f_{shear} = 0$  notes that the normal and shear stresses on a plane in a soil mass on failure envelope, yellow line in figure 5. The material is yielding state in this situation.
- $f_{tension} < 0$  or  $f_{shear} > 0$  notes a state of stress plotting as red zone in figure 5 that cannot exist, since the stresses outside failure

envelope, failure would have occurred before this condition was reached.

For a slope stability analysis problem, tensile failure should be first considered, because tension strength of soil material is usually much smaller than shear strength. If take *cut-through* of the tension failure zone and shear failure surface as definition of slope failure, compute process can be illustrated as figure 6. Definition of slope failure is discussed in the third subsection. Note that the procedure of tension failure and shear failure automatically included in FLAC program while the global failure need own judgment based on different definitions.

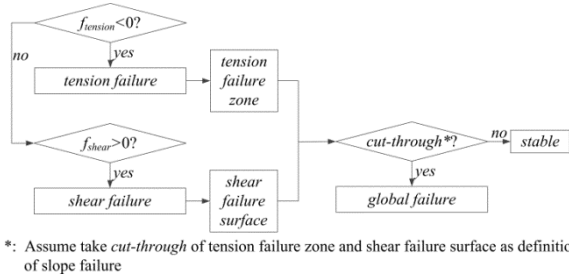


Figure 6 Flow chart of seismic slope stability analysis based on tension-shear failure mechanism

### 2.2 Factor of safety F and strength reduction factor SRF

Factor of safety  $F$  is a value that is used to examine the stability state of slopes and of great interest for engineering practice. A generally accepted definition of  $F$  is that first given by Bishop [31]: the ratio of the available strength of soil material to that required to maintain equilibrium. This definition used by Zienkiewicz [32], Ugai [20], Matsui & San [33], Griffiths & Lane [34], Dawson & Roth [35], Zheng et al. [21] and others. For  $c$ - $\phi$ - $\sigma_t$  material studied in this paper, factor of safety  $F$  against slope is simply calculated as

$$F = \frac{c}{c'} = \frac{\tan \phi}{\tan \phi'} = \frac{\sigma_t}{\sigma_t'} \quad (8)$$

where  $c$ ,  $\phi$  and  $\sigma_t$  are the actual values of soil material. They are cohesion, friction angle and tensile strength, respectively, and  $c'$ ,  $\phi'$  and  $\sigma_t'$  are the relevant parameters required to maintain the limit equilibrium. To achieve the correct factor of safety  $F$ , it is essential to trace the strength parameters by a coefficient called strength reduction factor  $SRF$  until the limit state of slope is achieved. The flow chart of calculation of factor of safety is shown in Figure 7. Strength reduction factor  $SRF$  defined as

$$SRF = \frac{c}{c_m} = \frac{\tan \phi}{\tan \phi_m} = \frac{\sigma_t}{\sigma_{tm}} \quad (9)$$

where  $c_m$ ,  $\phi_m$  and  $\sigma_{tm}$  are the calculated values of strength.



Figure 7 Flow chart of calculation of factor of safety

It should be note that factor of safety  $F$  and strength reduction factor  $SRF$  are two different concepts. Only when the slope is in limit equilibrium state, the value of  $SRF$  equals to factor of safety  $F$ .

### 2.3 Definition of slope failure

When strength reduction technique is used to analyze slope stability, one typical problem is how to define the state of slope failure. At present, in static situation, there are several possible definitions of slope failure in numerical simulation, e.g. *cut-through* of plastic zone from toe to top of slope, *non-convergence* of the solution [36], *mutation* of displacement of potential failure mass [37] and so on.

In static case, similar outcomes can be obtained based on these definitions of slope failure. Although these definitions of failure have been widely used in numerical simulation, it is difficult to implement with the current dynamic simulation. In dynamic numerical simulation, few studies focus on definition of slope failure was carried out. From the early researchers, three possible definitions of slope failure can be used in a dynamic analysis:

- (1) *Cut-through* of plastic zone from bottom to top surface of a slope,
- (2) *Non-convergence* of permanent displacement of potential failure mass, and
- (3) *Mutation* of permanent displacement of potential failure mass.

Note that, permanent displacement in these definitions of failure notes residual displacement after an earthquake event. In the example studied in here, the first definition of failure, *cut-through* of plastic zone from bottom to top surface of a slope, is taken as being key indicator of seismic slope failure. In addition, comparison of slope failure definitions on seismic slope stability analysis is presented in section 5.

## 3. DYNAMIC FORMULATION

### 3.1 Brief description of dynamic analysis using FLAC<sup>3D</sup>

The program used in this paper is finite difference program FLAC<sup>3D</sup> version 3.10 [38]. The calculation is based on the explicit finite difference scheme to solve the full equations of motion, using lumped grid point masses derived from the real density of surrounding zones rather than fictitious masses used for optimum convergence in the static solution scheme. And a flow chart of dynamic analysis for a slope is illustrated in figure 8.

In the whole process, there are several important aspects should be considered while preparing a FLAC model for dynamic analysis: in terms of (1) dynamic loading, (2) boundary conditions, (3) mechanical damping, and (4) wave transmission through the model. They are discussed in this section.

### 3.2 Modeling with FLAC<sup>3D</sup>

This paper analyzes a classical homogeneity slope with the height of 20m and the incline angle of 45° that has studied by some earlier researchers [21, 28]. A schematic illustration of the 2D analyzed mesh and the boundary conditions is provided in figure 9. In order to study the development process of slope failure surface, one square meters of grid size is meshed. Both  $x$  and  $y$  displacements are fixed at the base of the model. And  $x$  displacements are fixed on either side of the model along the  $y$ -axis. The slope is allowed free to move in both the directions. Free field boundary is used in the present model to minimize the wave reflection. This boundary condition provides a better representation when quiet boundaries are used in conjunction with external seismic sources. The size of slope ensures the assumption of free field boundary. For a dynamic analysis, FLAC<sup>3D</sup> version 3.10 program provides several mechanical damping in which local damping is a simple and pragmatic method. The local damping coefficient  $\alpha_L$  defined as

$$\alpha_L = \pi D \quad (10)$$

where  $D$  is fraction of critical damping. Although the actual value given to the local damping has a profound influence on the dynamic wave transmission, if it chooses from a certain range, it has little influence on the predicted factor of safety in seismic slope stability analysis. Hence, local damping of 0.157 (i.e. fraction of critical damping is 5%) is used in the model as suggested by other studies for these kinds of problems.

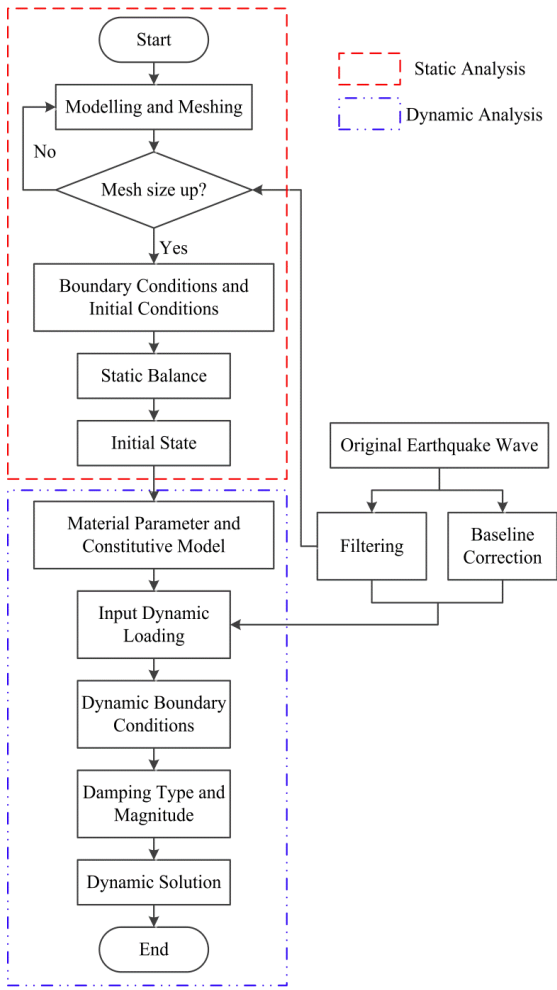


Figure 8 Flow chart of seismic slope stability analysis using FLAC program (Modified from [39]).

Table 2 shows the properties parameters of soil material used in the analysis. It should be note that some unlisted parameters e.g. unit weight  $\gamma$ , modulus of volume  $K$  and shear modulus  $G$ , are also used in this paper. They can be translated from the parameters listed in table 2. The density  $\rho$  assigned to the soil decides the total unit weight  $\gamma$  and to move forward the self-gravity load. The parameters

$c$  and  $\phi$  note the effective cohesion and inter friction angle of the soil material. The dilation angle  $\psi$  affects the volume change of the soil during yielding. In this study, we take  $\psi=\phi$ , i.e. the plasticity flow rule is associated and direct comparisons with theorems from classical plasticity can be made. In addition, it should be note that the tensile strength  $\sigma_t$  is taken as 0, because it is so unreliable that can be ignored.

Table 2 Property parameters of slope material

Parameters	Value
Modulus of elasticity $E$	$77.48 \times 10^6$ Pa
Poisson's ratio $\mu$	0.3
Density $\rho$	$2000 \text{ kg/m}^3$
Cohesion $c$	40000 Pa
Inter friction angle $\phi$	$20^\circ$
Dilation angle $\psi$	$20^\circ$
Tensile strength $\sigma_t$	0

### 3.3 Earthquake loading

#### 3.3.1 Original earthquake loading

The dynamic load applied in here is the transverse component of the acceleration time history (record name: KJM-0°) modified from the Kobe earthquake, occurred in Japan, 1997 as shown in Figure 10. The total duration of the earthquake loading is 15s with a time step of 0.02s. The  $a_{max}$  value of the recorded earthquake is 0.2046g at time of 3.52s. The earthquake loading is applied at bottom of the whole stratum. From the acceleration time history record, velocity and displacement time histories can be computed by once and twice integration respectively.

#### 3.3.2 Baseline correction

If the acceleration record shown in figure 10 is directly used as an earthquake loading time history, the FLAC<sup>3D</sup> model may exhibit continuing velocity or residual displacements after the motion has finished as shown in figure 11(a) and figure 11(b). This arises from the fact that the integral of the complete acceleration time history may not be zero. In this paper, a low frequency velocity wave which, when added to the original history, produces a final displacement which is zero is used. The action will not affect the mechanics of the deformation of the model. The process of baseline correction and corrected displacement time histories are shown in Figure 11.

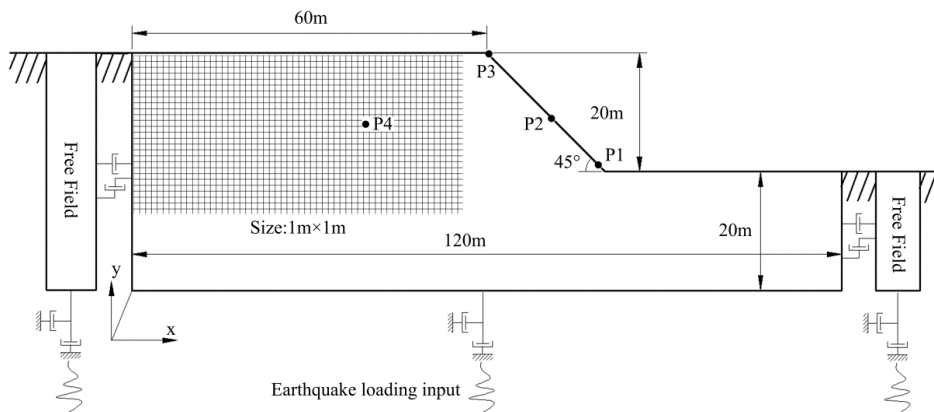


Figure 9 Mesh generation and boundary conditions of finite difference model for dynamic slope stability analysis.

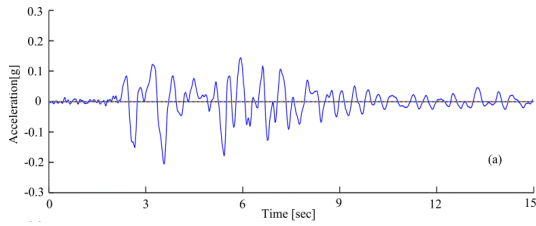


Figure 10 Acceleration time history of earthquake loading applied in study

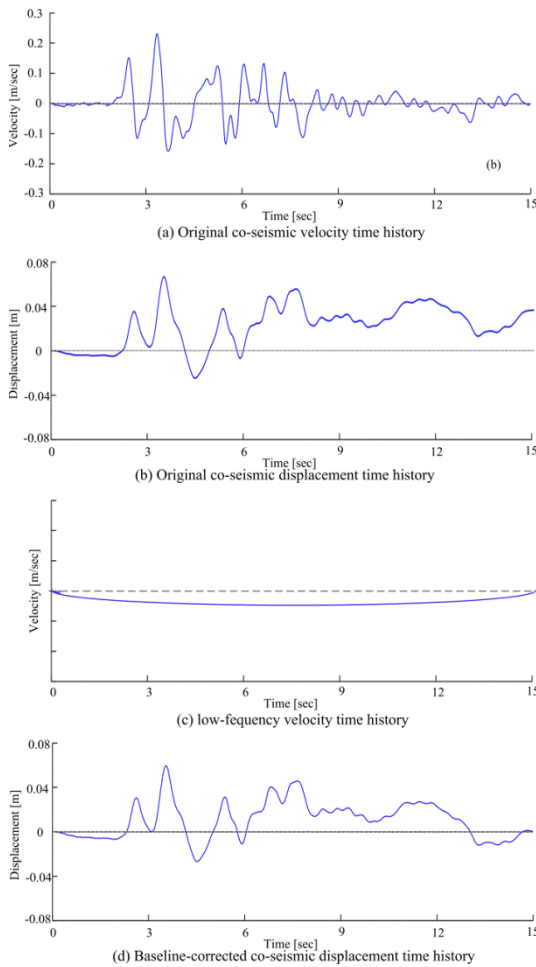


Figure 11 The baseline correction process

### 3.3.3 Translation of stress time history

In order to avoid the effect of the quiet boundary be nullified, a stress boundary condition is used. This stress history is transformed from a velocity record using the formula

$$\sigma_s = 2(\rho C_s)v_s \quad (11)$$

where  $C_s$  is the speed of  $s$ -wave propagation through medium;  $v_s$  is input shear particle velocity time history of earthquake loading. The factor of two in the equation accounts for the fact that the applied stress must be doubled to overcome the effect of the viscous boundary.  $C_s$  is given by

$$C_s = \sqrt{G / \rho} \quad (12)$$

where  $G$  is the shear modulus of material and given by

$$G = E / [2(1 + \mu)] \quad (13)$$

Figure 12 shows the input stress time history shifted from velocity time history.

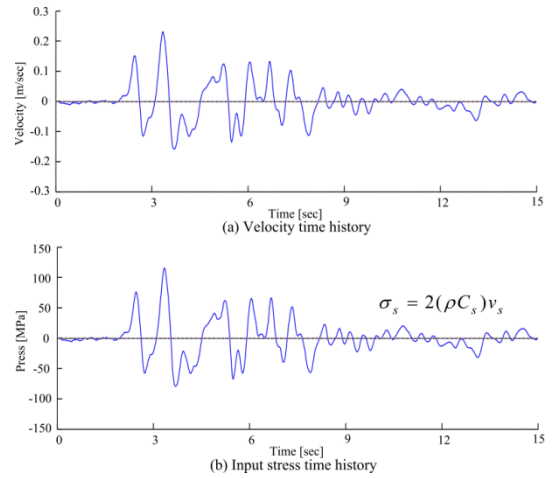


Figure 12 Input stress time history shifted from velocity time history. (a) Velocity time history shifted during single integration from original seismic accelerations; (b) Shifted stress time history from velocity time history

## 4. RESULTS

In this section, three major results of seismic slope stability analysis are presented. The first is the validation of stress state and relationship with tension failure. The second is about the permanent displacement in actual strength case. The third is the factor of safety under different failure mechanism and the forth aspect is the shape of slip surface.

### 4.1 Stress and tension failure

Figure 13 shows the major and minor principle stresses records of a monitoring point set away from the slope surface and with a certain depth from top surface in where the influence of wave reflection and refraction is small. From the figure, an opposite change pattern of major and minor principal stresses  $\sigma_1'$   $\sigma_3'$  can be found that consist with the description of section 2.1.

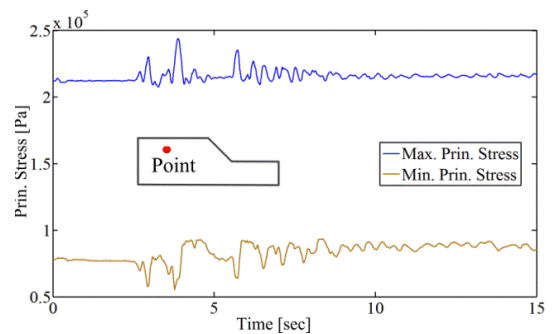


Figure 13 Principle stresses records of a point in slope under an earthquake loading

As previous yield criterion, tension-shear failure criterion, tension failure firstly judged based on the minor principle stress. The depth of tension failure zone can be judged. Figure 14 shows a serious minor principle stresses records of points that have different depth from top of slope. As the tension failure criterion, once the minor principle stress smaller than tensile strength of soil, tension failure will occur. In figure 14, black dash line notes tensile strength of soil material, stress records of points in depth of 1~5 m outstrip

the tensile strength line. So we can take the conclusion that depth of tension failure zone is 5~7m. Figure 15 shows the block tension state in which 5~7m depth of tension failure zone can be found.

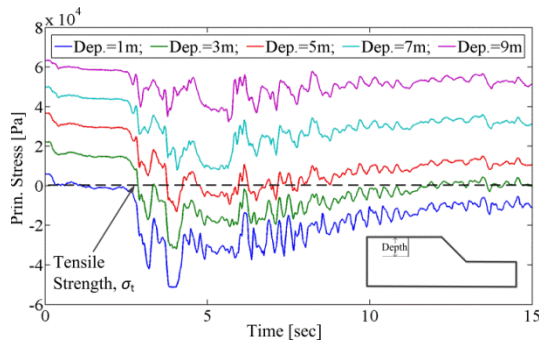


Figure 14 Minor principle stress records of monitoring points

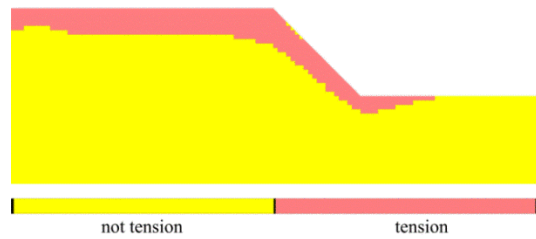


Figure 15 Tension state of slope after the shaking

#### 4.2 Permanent displacement

The contour of permanent displacement of the slope after the complete dynamic event is shown in figure 16. It can be found that a maximum displacement ( $D_{max}$ ) of 0.2896m is observed near the toe. This displacement is the accumulated permanent displacement due to earthquake. Figure 16 also depicts that the displacements are nearer to the toe of the slope.

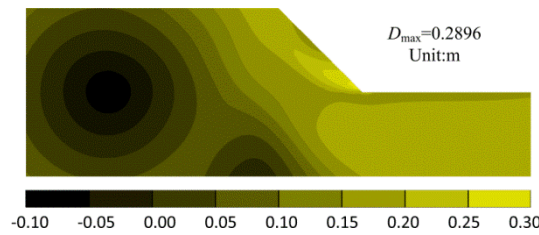


Figure 16 Contour of permanent displacement of the slope after the complete seismic event

In addition, the displacements along the slope face are captured using the *history* command in FLAC library. Typical variations of horizontal and vertical displacements with time at various monitoring points (see figure 9) during the earthquake are shown in figure 17 and figure 18, respectively. It can be seen from figure 10 that the horizontal permanent displacements are about 0.33m, 0.20m, 0.12m and 0.00m at points P1, P2, P3 and P4, respectively and with little change after the motion. It can be seen from figure 11 that the vertical permanent displacements are about 0.33m, 0.20m,

0.12m and 0.00m at points P1, P2, P3 and P4, respectively and with continue increase after the motion expect the point P4.

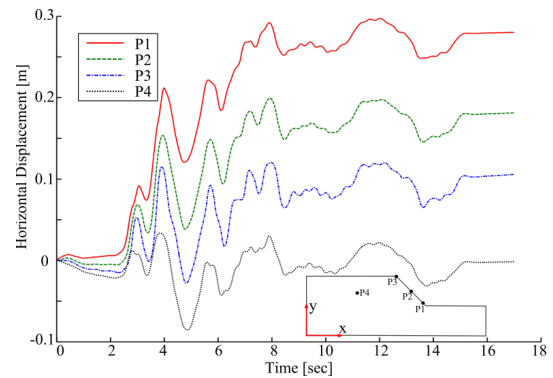


Figure 17 Horizontal displacement time histories of monitoring points

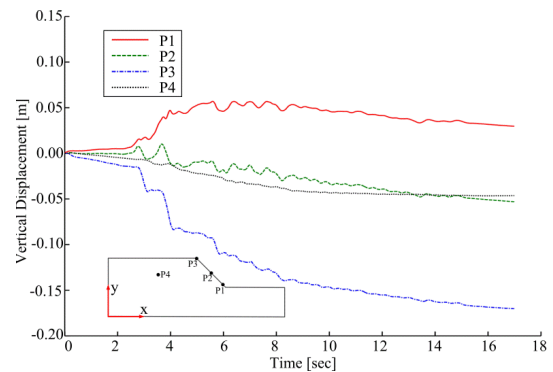


Figure 18 Vertical displacement time history of monitoring points

#### 4.3 Factor of safety $F$ based on tension-shear failure mechanism

As previous mentioned, factor of safety  $F$  can be computed by reducing the soil strength in stages to bring the slope into a state of limiting equilibrium. The stability analysis of slope is carried out based on tension-shear failure mechanism.

Take the *cut-through* of tension failure zone and shear failure surface as definition of seismic slope failure, the failure surface contains tension and shear segment. Tension segment depended on the depth of tension failure zone, and shear segment decided by the shear strain increment, i.e. cumulant of shear strain. After a series of trying calculation, it can be obtained that *cut-through* of tension plastic zone and shear failure zone occurred in the smallest  $SRF$  of 0.99. The figure 19 shows the contours of tension plastic zone and shear strain increment at situations of  $SRF=0.98$  and  $SRF=0.99$ . The maximum values of shear strain increment ( $SSI_{max}$ ) are 0.03219 and 0.03593, respectively. It can be found that the significant shear strain increment not increases to the tension zone at  $SRF=0.98$ , while *cut-through* of tension failure and shear failure is obtained at  $SRF=0.99$ . Hence, we can take the opinion that the slope is in the limit state at  $SRF=0.98$ . As the previous definition of factor of safety, it is 0.98 based on the tension-shear failure mechanism.

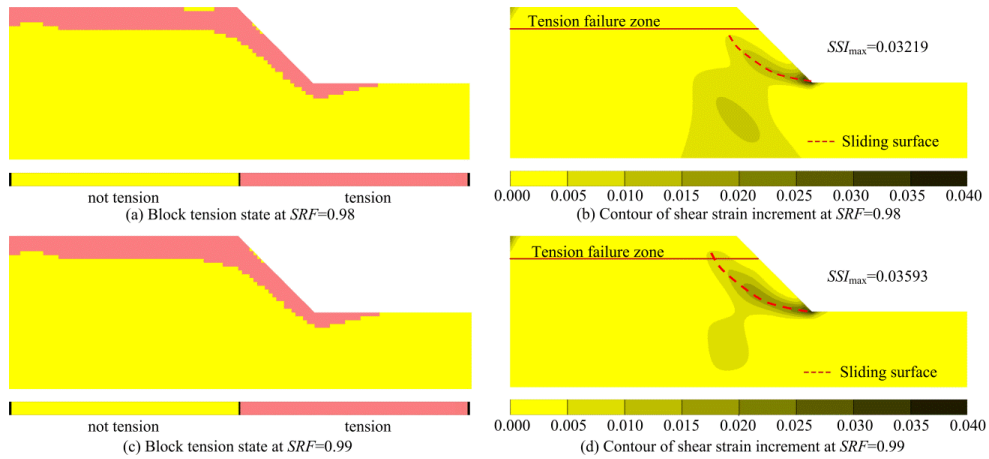


Figure 19 Block tension state and contour of shear strain increment at  $SRF=0.98$  and  $SRF=0.99$

5. COMPARISONS AND DISCUSSIONS

5.1 Traditional failure mechanism: completely shear failure

If only consider the shear failure mechanism, failure surface of slope is just induced by the shear failure. Take the *cut-through* of shear plastic zone as definition of seismic slope failure as well, after a series of trying calculation, it can be obtained that *cut-through* of shear plastic zone occurred in the smallest  $SRF$  of 1.12. The figure 20 shows the contours of shear strain increment at  $SRF=1.11$  and  $SRF=1.12$ , respectively. The maximum values of shear strain increment ( $SSI_{max}$ ) are 0.07264 and 0.07963 at  $SRF=1.11$  and  $SRF=1.12$ , respectively. These results show that the slope is in the limit state at the situation of  $SRF=1.11$ . As the previous definition of factor of safety and the *cut-through* definition of slope failure, we can come to the conclusion that factor of safety  $F$  is 1.11 based on single shear failure mechanism.

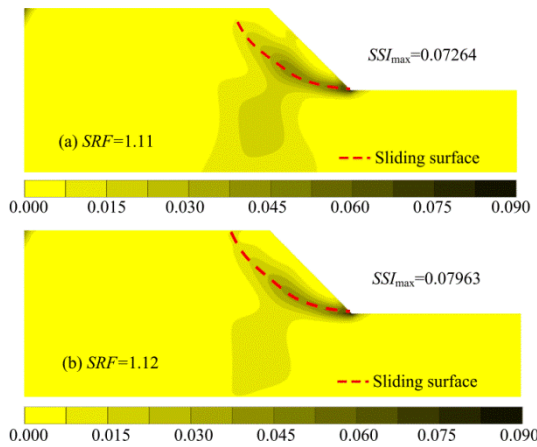


Figure 20 Contours of shear strain increment at (a)  $SRF=1.11$  and (b)  $SRF=1.12$

The factor of safety 1.11 calculated based on traditional failure mechanism is larger than that 0.98 based on tension-shear failure mechanism. For the studied slope in here, factor of safety reduce about 12% from traditional failure mechanism to new failure mechanism, i.e. tension-shear failure mechanism.

According to the previous analysis, different factor of safety  $F$  are obtained from different failure mechanism. In order to provide evidence for the correctness of tension-shear failure mechanism, the second definition of slope failure, *non-convergence* of permanent displacement of potential failure mass, is used in here. Permanent displacements of potential failure mass are recorded by set some key monitoring points along the surface of slope (see Figure 9). Horizontal velocity and displacement time histories of three monitoring points at  $SRF=1.11$  and  $SRF=0.98$  are proposed in

figure 21~24. From Figure 21, we can found that the residual velocity of monitoring points after the shaking is not equals zero at  $SRF=1.11$ , and from Figure 22, *non-convergence* of permanent displacement also be proposed, i.e. the slope is not stable at  $SRF=1.11$ . In opposite, Figures 23 and 24 show the velocity that equals to 0 and convergence of permanent displacement, respectively, i.e. the slope is stable at  $SRF=0.98$ . These results confirm the correctness and reasonable of tension-shear failure mechanism.

5.2 Definition of seismic slope failure

As previous description, there are three definitions of slope failure can be considered in a dynamic analysis. The previous analysis mainly used the first definition. Some researcher have used the other two definitions for seismic slope stability analysis and obtained some useful results, but research of definition of seismic slope failure is still in primary stage and much research should be done to certify the correctness and applicability of every definitions. Based on the example studied in here, primary discussion is given below.

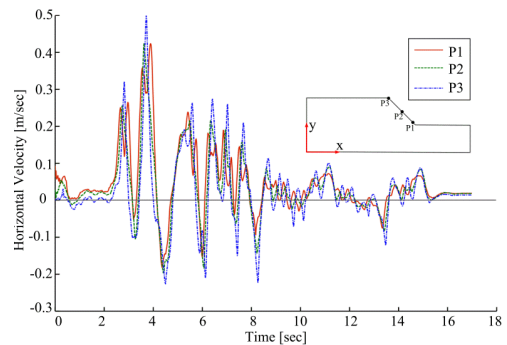


Figure 21 Horizontal velocity records of monitoring points at slope surface at  $SRF=1.11$

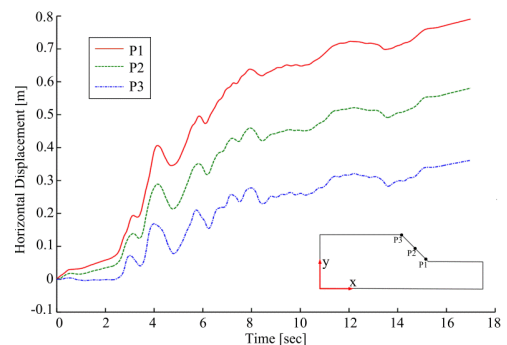


Figure 22 Horizontal displacement records of monitoring points at slope surface at  $SRF=1.11$

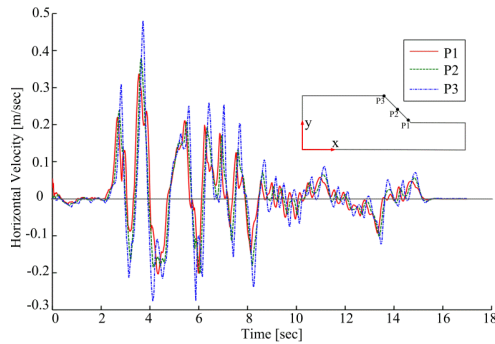


Figure 23 Horizontal velocity records of monitoring points at slope surface at  $SRF=0.98$

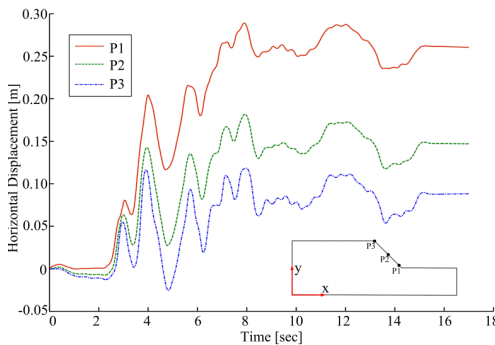


Figure 24 Horizontal displacement records of monitoring points at slope surface at  $SRF=0.98$

### 5.2.1 Non-convergence of permanent displacement of potential failure mass

Figure 25 shows the horizontal displacement time histories of key point P1 under different strength reduction factor  $SRF$ . The permanent displacements after motion at  $SRF=0.90\sim 1.30$  show a change of from convergence to non-convergence. If take the *non-convergence* of permanent displacement as definition of seismic slope failure, from the Figure 25, we can found that factor of safety  $F$  of the studied slope should be a value between  $0.95\sim 1.02$  that consist with the result of *cut-thought* definition of slope failure consider tension-shear failure mechanism. Other monitoring points, e.g. P2, P3, have the same change trend.

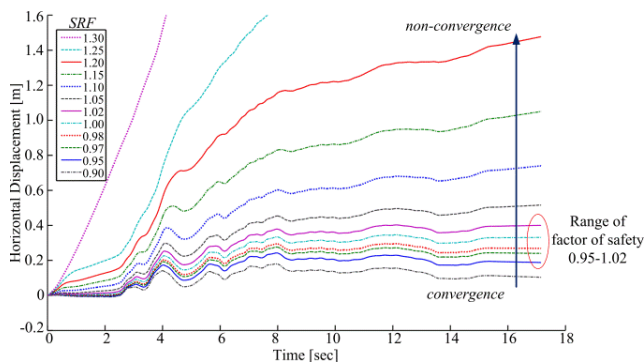


Figure 25 Horizontal displacement records of monitoring point at toe of slope at  $SRF=0.90\sim 1.30$

### 5.2.2 Mutation of permanent displacement of potential failure mass

If take *mutation* of permanent displacement of potential failure mass as the definition of seismic slope failure, only need to record the residual displacements of monitoring points after the seismic event. Figure 26 shows the horizontal residual displacement of monitoring points at different strength reduction factor  $SRF$ . From the figure 26, it can be found that the residual displacement increase

exponentially with the increase of  $SRF$  and mutate at  $SRF=1.28\sim 1.30$ . As the third definition of slope failure, the factor of safety should be 1.28. Compare to the results from other reliable methods, we can clearly found that the *mutation* definition of seismic slope failure is not reliable in some situation, e.g. the slope studied in here.

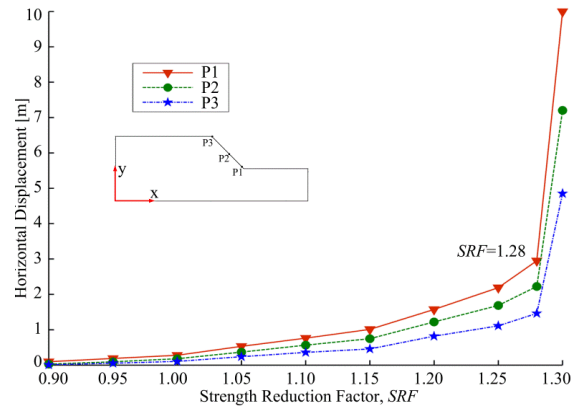


Figure 26 Horizontal permanent displacement of monitoring points at slope surface at  $SRF=0.90\sim 1.30$

Based on the above discussion, the authors recommend the first two definitions of slope failure and take the influence of tension failure.

### 5.3 Shape of slip surface

The shape of slip surface is an important aspect of seismic slope stability analysis. Because it has a close relationship with volume of slip mass that plays a determination role on the starting velocity and travel distance once slope collapse occurred and formed a landslide. The Figure 27 shows the failure surfaces of slope in different cases: static case, dynamic cases based on shear mechanism and tension-shear mechanism. From the figure 27, we can found that in dynamic cases, shapes of slip surface are shallower than that under static case (dense green dotted line). More important, the failure surface under tension-shear failure mechanism (blue solid line) contains two segments: tension failure and shear failure which consist with the result of model test [23, 40] and post-earthquake investigation [24, 26].

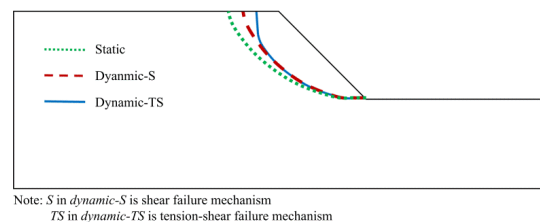


Figure 27 Failure surfaces under static and dynamic situations based on different failure mechanisms

### 5.4 Comparison of factor of safety

As previous description, the calculation of factor of safety  $F$  is one of the most important aspects of seismic slope stability analysis. The Table 3 shows the factors of safety  $F$  from various methods. From the Table 3, it can be found that the result presented in this paper similar with those obtained from pseudo-static method. The results based tension-shear failure mechanism is reasonable and smaller than that obtained from traditional single shear failure mechanism.

5.5 Progressive failure

The failure progress of slope has an important significance for design of reinforce slope against earthquake loading. Considering the tension-shear failure mechanism, the Figure 28 shows the failure progress of seismic slope at different dynamic time. From the Figure 28, it can be obviously found that the instability of slope is a progressive failure in which the shear failure zone is expand slowly from the toe upward to the top of slope and achieve a *cut-through* with tension failure zone. In this example, the slope is not collapse at dynamic time  $t=3s$  at which the first peak of wave of the earthquake loading go through. After the largest peak of wave shaking at time of  $6s$ , the slope have a significant performance but the cut-through of tension zone and shear failure zone is not achieved. The global instability occurred at time  $t=9s$  at which the largely peak of wave have went through. From the figure of tension state of block, we can found that the tension failure occurred at time of largest peak of wave go through. It should be noted that the result presented here is just a tentative results. The research of tension failure mechanism of seismic slope is at the primary stage and there is still plenty work to do.

Table 3 Factors of safety  $F$  calculated from various methods.

Method		$F$
Static situation		1.27*
Pseudo-static method <sup>a</sup>	$k=PGA$	$TS^b$
		$S^c$
	$k=1/2PGA$	$TS$
		$S$
Present method	$Cut-through^d$	0.98
	$Non-convergence^e$	0.95~1.02
	$Mutation^f$	1.28

\* The result is calculated using limit analysis method  
 \*\* The results are calculated using limit analysis method presented in reference [29]  
<sup>a</sup>  $k$  is pseudo-static seismic coefficient, PGA is peak ground acceleration  
<sup>b</sup> TS notes tension-shear failure mechanism  
<sup>c</sup> S notes shear failure mechanism  
<sup>d e f</sup> Note three definitions of slope failure presented in section 2

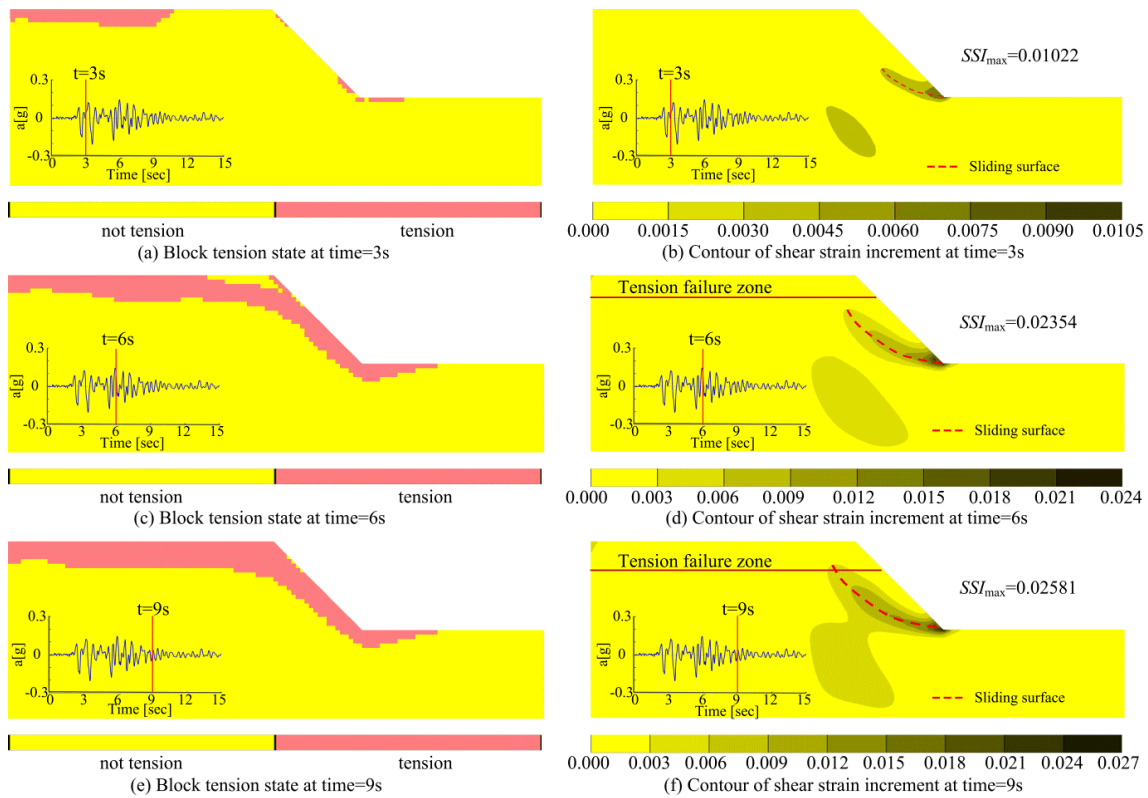


Figure 28 Process of seismic slope failure.

6. CONCLUSION

This paper analyzed the stability of seismic slope using the finite difference program FLAC<sup>3D</sup>. Based on the analysis above, the following main conclusions are drawn:

- 1) Tension failure has a significant influence on seismic slope stability analysis. The FLAC<sup>3D</sup> program can take the influence of tension failure into consideration, so as to make the analysis technique more reasonable for practical application. It can be used to determine reasonable factor of safety  $F$  which smaller than that obtained from traditional single shear failure mechanism. The widespread use of this mechanism should now be seriously considered to traditional failure mechanism.
- 2) Definition of failure is an important aspect in seismic slope stability analysis. As the example studied in here, *non-convergence* of permanent displacement of potential failure mass is a reliable

definition of seismic slope failure. If take the influence of tension failure into consideration, the first definition of failure, *cut-through* of plastic zone from bottom to top surface of a slope under tension-shear failure mechanism, gives results very similar to the second definition of failure, *non-convergence*. In addition, the third definition of slope failure can resulted in unreasonable outcome.

3) The shapes of failure surface of seismic slope under traditional single shear failure mechanism and tension-shear failure mechanism have an obvious difference. Failure surface of seismic slope considering tension-shear failure mechanism contains two segments and shallower than that just considering the shear failure while ignoring the influence of tension failure.

4) The failure of seismic slope is progressive with the proceeding of earthquake. The instability of slope is a progressive failure in which the shear failure zone is expand slowly from the toe

upward to the top of slope and achieve a cut-through with tension failure zone.

It should be noted that seismic slope stability analysis is a complex problem, especially about the seismic slope failure mechanism. The conclusions listed in here are based on limited observations. More in-depth and more extensive research should continue to be studied in future.

## 7. ACKNOWLEDGMENTS

This study has received financial support from the Global Environment Research Fund of Japan (S-8), and from Grants-in-Aid for Scientific Research (Scientific Research (B), 22310113, G. Chen) from Japan Society for the Promotion of Science. And the first author acknowledges the support of China Scholarship Council. These financial supports are gratefully acknowledged.

## 8. REFERENCES

- Bishop, A.W., The use of slip circle in the stability analysis of slopes, *Geotechnique*, 4 (1955) 7-17.
- Bray, J.D., Rathje, E. M., Earthquake-induced displacements of solid-waste landfills, *J Geotech Geoenviron*, 124 (1998) pp242-253.
- Bray, J.D., Travarasou, T., Simplified procedure for estimating earthquake-induced deviatoric slope displacements, *J Geotech Geoenviron*, 133 (2007) 381-392.
- California Department of Conservation, Division of Mines and Geology, Guidelines for evaluating and mitigating seismic hazards in California, CDMG Special Publication, 1997, pp117.
- Chen, Y.M., Xu, D.P., *FLAC/FLAC3D foundation and engineering project*, China WaterPower Press, Beijing, China, 2009. (in Chinese)
- Chopra, A.K., The importance of vertical component of earthquake motion, *Bull Seism Soc Am*, 56 (1966) pp1163-1175.
- Dai, F., Xu, C., Yao, X., Xu, L., Tu, X., Gong, Q., Spatial distribution of landslides triggered by the 2008 Ms 8.0 Wenchuan earthquake, China, *J Asian Earth Sci*, 40 (2011) pp883-895.
- Dawson, E.M., Roth, W.H., Drescher, A., Slope stability analysis by strength reduction, *Geotechnique*, 49 (1999) 835-840.
- Griffiths, D.V., Lane, P.A., Slope stability analysis by finite elements, *Geotechnique*, 49 (1999) 387-403.
- Huang, R.Q., et al., *Geohazard Assessment of the Wenchuan Earthquake*, Science Press, Beijing, China, 2009. (in Chinese)
- Huang, R.Q., Xu, Q., Huo, J., Mechanism and geo-mechanics models of landslides triggered by 5.12 Wenchuan earthquake, *J Mountain Sci*, 8 (2011) 200-210.
- Hyness-Griffin, M.E., Franklin, A.G., Rationalizing the seismic coefficient method, Miscellaneous Paper GL-84-13, U.S. Army Corps of Engineers Waterways Experimental Station, Vicksburg, Mississippi, 1984, pp21.
- Itasca, *FLAC<sup>3D</sup> fast Lagrangian analysis of continua in 3 dimensions V.2.0*, Itasca Consulting Group, Inc., Minneapolis.
- Jibson, R.W., Methods for assessing the stability of slopes during earthquakes—A retrospective, *Eng Geol*, 122 (2011) pp43-50.
- Latha, G.M., Garaga, A., Seismic stability analysis of a Himalayan rock slope, *Rock Mech Rock Eng*, 43 (2010) 831-843.
- Lin, J.S., Whitman, R.V., Earthquake induced displacements of sliding blocks, *J Geotech Eng*, 112 (1983) 44-59.
- Lin, M.L., Wang, K.L., Seismic slope behavior in a large-scale shaking table model test, *Eng Geol*, 86 (2006) 118-133.
- Ling, H.I., Leshvinsky, D., Effects of vertical acceleration on seismic design of geosynthetic-reinforced soil structures, *Geotechnique*, 48 (1998) 347-373.
- Makdisi, F.I., Seed, H.B., Simplified procedure for estimating dam and embankment earthquake-induced deformations, *ASCE J of Geotech Eng Div*, 104 (1978) 849-867.
- Marcuson, W.F., Moderator's report for session on Earth Dams and Stability of Slopes under Dynamic Loads. Proceedings, International Conference on Recent Advances in Geotechnical Earthquake Engineering and Soil Dynamics, St. Louis, MO, 3, 1981, pp1175.
- Matsui, T., San, K.C., Finite element slope stability analysis by shear strength reduction technique, *Soils Found*, 32 (1992) 59-70.
- Newmark, N.M., Effects of earthquakes on dams and embankments, *Geotechnique*, 15 (1965) 139-159.
- Pyke, R.M., Selection of seismic coefficients for use in pseudostatic slope stability analyses, <http://www.tagasoft.com/TAGAsoft/TAGAsoft/Discussion/article2.html>.
- Rathje, E.M., Bray, J.D., An examination of simplified earthquake-induced displacement procedures for earth structures, *Canadian Geotech J*, 36 (1999) 72-87.
- Rathje, E.M., Bray, J.D., Nonlinear coupled seismic sliding analysis of earth structures, *J Geotech Geoenviron*, 126 (2000) 1002-1014.
- Seed, R.B., Considerations in earthquake-resistant design of earth and rockfill dams, Nineteenth Rankin Lecture, *Geotechnique*, 29 (1979) pp13-41.
- Stewart, J.P., Blake, T.F., Hollingsworth, R.A., A screen analysis procedure for seismic slope stability, *Earthq Spectra*, 19 (2003) pp697-712.
- Terzaghi, K., *From Theory to Practice in Soil Mechanics: selections from the writings of Karl Terzaghi, with bibliography and contributions on his life and achievements*, L. Bjerrum, et al. (Eds.), New York, John Wiley and Sons, 1960, pp. 202-245.
- Ugai, K., A method of calculation of total safety factor of slopes by elasto-plastic FEM, *Soils Found*, 29 (1989) 190-195. (in Japanese)
- Wakai A, Ugai K, Sato M, and Tazo T. "Numerical analysis for seismic behavior of a slope based on a simple cyclic loading model," 4th International Conference on Recent Advances in Geotechnical Earthquake Engineering and Soil Dynamics, Paper No. 5.06 in CD-ROM, San Diego.
- Xu, Q., Pei, X.J., Huang, R.Q., et al. *Large-scale landslides induced by the Wenchuan earthquake*, Science Press, ISBN 978-7-03-026906-5, Beijing, China, 2009. (in Chinese)
- Yan, Z.X., Zhang, S., Zhang, X.D., Duan, J., Failure mechanism and stability analysis of slope under earthquake, *J Eng Geol*, 18 (2010) 844-849. (in Chinese)
- Yin, Y.P., Wang, F.W., Sun, P., Landslide hazards triggered by the 2008 Wenchuan earthquake, Sichuan, China, *Landslides*, 6 (2009) 139-152.
- Zhang, Y.B., Chen, G.Q., Zen, K., Kasama, K., Dong, S.M., Limit analysis of seismic slope stability based on tension-shear failure mechanism, Proceedings, Slope Stability 2011: International Symposium on Rock Slope Stability in Open Pit Mining and Civil Engineering. 18-21, September 2011 Vancouver, Canada.
- Zhang, Y.B., Chen, G.Q., Zen, K., Kasama, K., Wu, J., Zheng, L., Seismic slope stability analysis subjected to tension failure, Western Regional Division Report of Natural Disaster Research Council, No. 36 (2012) 21-24.
- Zheng, Y.R., Tang, X.S., Zhao, S.Y., Deng, C.J., Lei, W.J., Strength reduction and step-loading finite element approaches in geotechnical engineering, *J Rock Mech and Geotech Eng*, 1 (2009) 21-30.
- Zienkiewicz, O.C., Humpheson, C., Lewis, R.W., Associated and non-associated visco-plasticity and plasticity in soil mechanics, *Geotechnique*, 25 (1975) 671 - 689.
- Zienkiewicz, O.C., Taylor, R.L., *The finite element method*, Vol.1, 4<sup>th</sup> edn, London, New York: McGraw-Hill, 1989.